Sporadic driving of dynamical systems

Toni Stojanovski,[1] Ljupčo Kocarev,[2] Ulrich Parlitz,[3] and Richard Harris[1]
[1]*CATT Centre, 723 Swanston Street, RMIT University, Melbourne, Australia*
[2]*Department of Electrical Engineering, Ss Cyril and Methodius University, 91000 Skopje, P.O. Box 574, Republic of Macedonia*
[3]*Drittes Physikalisches Institut, Universität Göttingen, Bürgerstraße 42-44, D-37073 Göttingen, Germany*
(Received 16 July 1996; revised manuscript received 22 November 1996)

In this paper the sporadic driving of time continuous systems and accompanying phenomena are examined. Mathematical analysis of sporadically driven linear systems gives an explanation for the observed dependence of the asymptotic stability of the sporadically driven system on the driving period. Several generalizations of sporadic driving are proposed and their practical implications are considered. The sensitivity of the synchronized motion between sporadically coupled chaotic systems to the influence of noise is explored. The synchronization test of nonlinear models for time series is enhanced through the usage of sporadic driving. [S1063-651X(97)02804-3]

PACS number(s): 05.45.+b

I. INTRODUCTION

Nowadays it is well known [1] that even for dynamical systems behaving chaotically, one can find subsystems which possess the property of asymptotic stability. Asymptotic stability of the driven subsystem is a necessary and sufficient condition for synchronization of the subsystem to the driving chaotic system [1,2]. Initially, the idea of synchronized chaotic motions seemed surprising and a bit paradoxical due to the sensitive dependence upon initial conditions. Since then, several researchers have contributed to the area and interesting results have emerged: synchronization of hyperchaotic systems and one directionally coupled one-dimensional arrays of chaotic systems connected with a scalar signal [3–6], transmission of information signals between synchronized chaotic systems [3,5–9], generalized synchronization [10–12], etc.

In [13], the asymptotic stability of dynamical systems which are driven by random forces at regular intervals was investigated. On the basis of numerical simulations it was conjectured that, for a class of randomly driven dynamical systems, the final trajectory of the system is completely independent of the initial state provided that the time interval between two adjacent kicks by the random force is smaller than a certain threshold value. In [14], it was reported that synchronized motion between two identical one directionally coupled dynamical systems can be achieved when certain variables of the driven system are set to the corresponding variables of the driving system only at discrete times. More generally, in [15] it was shown that the asymptotic stability of a time continuously driven dynamical system implies asymptotic stability of the time discontinuous driven counterpart for sufficiently small driving periods. In other words, under certain conditions it is sufficient to drive a (chaotic) dynamical system only in time-equidistant moments in order to achieve its asymptotic stability, and not continuously as time goes on. In [15], the time discontinuous driving of dynamical systems was named *sporadic driving*. The possible applications of sporadic driving in communications were pointed out and analyzed to a certain extent. Sporadic driving enables the perfect transmission of chaotic signals through bandlimited channels. It was also shown how to realize a digital communication system on the basis of sporadic driving. Living in the era of digital communications, this might be an interesting and significant application of chaotic systems. The concept of sporadic driving may also be applied to synchronizing dynamical systems that are coupled by a signal that consists of spike trains. This case may, for example, occur with firing neurons or coupled lasers that interact with a (chaotic) sequence of sharp intensity pulses [16]. Although being physically connected continuously by some synapses or fiber optics, there is practically no interaction *between* the spikes and, therefore, the case of sporadic driving is (at least approximately) realized.

In this paper, we analyze the properties and the mechanism of asymptotic stability of sporadically driven systems. Clear understanding of the origins of asymptotic stability of sporadically driven systems is of great significance for the previously mentioned and some new applications that will possibly emerge in the future.

In Sec. II we shall summarize the achieved results regarding the idea of time discontinuous driving of dynamical systems and pose several relevant questions. Section III gives answers to these questions through mathematical analysis of linear examples, and points to some interesting phenomena. These phenomena are also encountered in sporadically driven nonlinear systems, as is shown in Sec. IV through numerical analysis. Section V contains generalizations of sporadic driving in different directions. Implications of the proposed generalizations for practical applications of sporadic driving are considered. In light of the latest results on the performance of the synchronized motion in a noisy environment, Sec. VI addresses this issue for the case of sporadically coupled chaotic systems. Section VII shows how sporadic driving can be used to test nonlinear models of experimental data. In Sec. VIII we summarize and make some concluding remarks.

II. SPORADIC DRIVING

The idea of asymptotic stability of time continuous dynamical systems that are time discontinuously driven has

been discussed by several authors [13–15]. In order to avoid any possible terminology ambiguities, at the beginning we define *stable*, *asymptotically stable*, and *unstable* driven dynamical systems.

Definition 1. Consider a driven dynamical system

$$\dot{\boldsymbol{x}}=\boldsymbol{G}(\boldsymbol{x},\boldsymbol{s}(t)), \tag{1}$$

where $\boldsymbol{x}\in\mathcal{U}_x\subseteq\mathcal{R}^N,\boldsymbol{s}\in\mathcal{U}_s\subseteq\mathcal{R}^M,\boldsymbol{G}:\mathcal{U}_x\times\mathcal{U}_s\rightarrow\mathcal{R}^N$. We say that Eq. (1) is *stable* with respect to the driving signal $\boldsymbol{s}(t)$ if there exists a phase point $\boldsymbol{x}_{0,1}$, such that for all $\varepsilon>0$ and t_0, a $\delta(\varepsilon,t_0)>0$ can be found such that $\|\boldsymbol{x}_{0,1}-\boldsymbol{x}_{0,2}\|<\delta(\varepsilon,t_0)$ implies

$$\|\boldsymbol{x}(t;t_0,\boldsymbol{x}_{0,1})-\boldsymbol{x}(t;t_0,\boldsymbol{x}_{0,2})\|<\varepsilon \quad \text{for } t>t_0. \tag{2}$$

The set $\mathcal{B}(\varepsilon,t_0)$ of all phase points $\boldsymbol{x}_{0,2}$ that satisfy Eq. (2) is called the *region of stability* of Eq. (1). If Eq. (1) is not stable then it is called *unstable*.

Definition 2. Consider Eq. (1). We say that Eq. (1) is *asymptotically stable* with respect to the driving signal $\boldsymbol{s}(t)$ if (i) Eq. (1) is stable with respect to the driving signal $\boldsymbol{s}(t)$; (ii) there exists a phase point $\boldsymbol{x}_{0,1}$ and a positive number $\delta(t_0)$, such that $\|\boldsymbol{x}_{0,1}-\boldsymbol{x}_{0,2}\|<\delta(t_0)$ implies

$$\lim_{t\rightarrow\infty}\|\boldsymbol{x}(t;t_0,\boldsymbol{x}_{0,1})-\boldsymbol{x}(t;t_0,\boldsymbol{x}_{0,2})\|=0. \tag{3}$$

The set $\mathcal{B}(t_0)$ of all phase points $\boldsymbol{x}_{0,2}$ that satisfy Eq. (3) is called the *region of asymptotic stability* of Eq. (1).

In simple terms, a driven dynamical system is asymptotically stable if it possesses asymptotically stable solutions. Some of these solutions may be different, i.e., $\lim_{t\rightarrow\infty}\|\boldsymbol{x}(t;t_0,\boldsymbol{x}_{0,1})-\boldsymbol{x}(t;t_0,\boldsymbol{x}'_{0,1})\|\neq 0$, where both $\boldsymbol{x}(t;t_0,\boldsymbol{x}_{0,1})$ and $\boldsymbol{x}(t;t_0,\boldsymbol{x}'_{0,1})$ denote asymptotically stable solutions. Different asymptotically stable solutions have different regions of asymptotic stability. In Definition 2 $\boldsymbol{x}_{0,2}$ denotes one phase point which belongs to the region of asymptotic stability of the solution $\boldsymbol{x}(t;t_0,\boldsymbol{x}_{0,1})$.

In this paper we shall consider the driven dynamical system (1) when its driving signal is applied only at equidistant time points $t_n=nT,n=\ldots,-1,0,+1,\ldots$, in the following manner: Decompose the state vector $\boldsymbol{x}$ into two parts $\boldsymbol{u}=[x_1,\ldots,x_M]$ and $\boldsymbol{v}=[x_{M+1},\ldots,x_N]$. At times t_n the components $\boldsymbol{u}$ are forced to new values $\boldsymbol{s}(t_n)$, that is, $\boldsymbol{u}(t_n)=\boldsymbol{s}(t_n)$. In the time intervals $t_n<t<t_{n+1}$, Eq. (1) behaves in an undriven way and free from the driving signal $\boldsymbol{s}(t)$. For this kind of *sporadic driving* only the values of $\boldsymbol{s}(t)$ at the time points t_n are relevant for the behavior of Eq. (1). Therefore, we say that Eq. (1) is driven by the time sequence $\boldsymbol{s}_T=\{\boldsymbol{s}(t_n)\}$ (note the usage of the subscript T). Sporadic driving of Eq. (1) as described in this paragraph can be mathematically written as

$$\dot{\boldsymbol{u}}=\boldsymbol{F}_u(\boldsymbol{u},\boldsymbol{v})+\sum_{n=-\infty}^{+\infty}\delta(t-t_n)(\boldsymbol{s}(t_n)-\boldsymbol{u}(t_{n-})),$$

$$\dot{\boldsymbol{v}}=\boldsymbol{F}_v(\boldsymbol{u},\boldsymbol{v}), \tag{4}$$

where $\delta(t)$ denotes a Dirac pulse, $\boldsymbol{u}(t_{n-})$ are the values of the signal $\boldsymbol{u}(t)$ immediately prior to the driving times t_n, and $\boldsymbol{F}_u=[f_1,\ldots,f_M]$ and $\boldsymbol{F}_v=[f_{M+1},\ldots,f_N]$ are a decomposition of the vector field $\boldsymbol{F}$ that governs the evolution of Eq. (4) in the time intervals $t_n<t<t_{n+1}$. Integrating Eq. (4) from time $t=nT-\varepsilon$ to $t=nT+\varepsilon$, one can find in the limit $\varepsilon\rightarrow 0$ that Eq. (4) describes a dynamical system which is sporadically driven by $\boldsymbol{s}_T$. For $T=0$ the sporadically driven system (4) becomes a time continuously driven system, i.e., the sporadic driving reduces to the driving method of Pecora and Carroll [1]

$$\boldsymbol{u}=\boldsymbol{s},$$

$$\dot{\boldsymbol{v}}=\boldsymbol{F}_v(\boldsymbol{u},\boldsymbol{v}). \tag{5}$$

One can check the asymptotic stability of any (time continuously or time discontinuously) driven system (1) numerically through conditional Lyapunov exponents (CLE), or analytically through a properly defined Lyapunov function. The CLEs of Eq. (4) depend not only on the vector field $\boldsymbol{F}$ and the driving signal $\boldsymbol{s}_T$, but also on the driving period T, since T is one of the defining parameters of Eq. (4). Therefore, CLEs of Eq. (4) will vary with T and will differ from those of Eq. (5), but their negativity is still a valid criterion for the asymptotic stability. This will be illustrated numerically and analytically in this paper. In [14] it was observed that despite the presence of a positive CLE of Eq. (5), it is still possible to achieve asymptotic stability of Eq. (4) for certain $T>0$ values.

The following theorem determines the conditions for asymptotic stability of sporadically driven dynamical systems. Its proof also explains the mechanism of asymptotic stability of sporadically driven systems.

Theorem. Consider the driven systems (4) and (5). If Eq. (5) is asymptotically stable, then the sporadically driven system (4) is asymptotically stable for sufficiently small driving periods T.

Proof: Denote with $\mathcal{B}$ the region of asymptotic stability of Eq. (5). Consider two copies of Eq. (5) driven by the same signal $\boldsymbol{s}(t)$ and starting from nearby initial conditions $\boldsymbol{v}_0,\boldsymbol{v}'_0\in\mathcal{B}$, and the $\boldsymbol{v}$ components $\boldsymbol{v}(t;t_0,\boldsymbol{v}_0)$ and $\boldsymbol{v}'(t;t_0,\boldsymbol{v}'_0)$ of their trajectories. The primed variables are from the second copy of Eq. (5). The evolution of the difference $\Delta\boldsymbol{v}(t)=\boldsymbol{v}(t;t_0,\boldsymbol{v}_0)-\boldsymbol{v}'(t;t_0,\boldsymbol{v}'_0)$ in the limit of small $\Delta\boldsymbol{v}$ is governed by

$$\Delta\dot{\boldsymbol{v}}=\boldsymbol{D}_v\boldsymbol{F}_v(\boldsymbol{s},\boldsymbol{v})\Delta\boldsymbol{v} \tag{6}$$

where $\boldsymbol{D}_v\boldsymbol{F}_v$ is the Jacobian of the vector field $\boldsymbol{F}_v$ with respect to the variables $\boldsymbol{v}$, and the higher-order terms $\boldsymbol{o}(\boldsymbol{s},\boldsymbol{v},\boldsymbol{v}')$ are neglected. Due to the assumed asymptotic stability of Eq. (5) it follows that $\lim_{t\rightarrow\infty}\|\Delta\boldsymbol{v}(t)\|=0$. In terms of CLEs, averaging Eq. (6) over the attractor will yield negative CLEs of $\dot{\boldsymbol{v}}=\boldsymbol{F}_v(\boldsymbol{s},\boldsymbol{v})$ with respect to $\boldsymbol{s}$ for all initial conditions $\boldsymbol{v}_0\in\mathcal{B}$.

Now consider two copies of the sporadically driven system (4) which are driven by the sampled version $\boldsymbol{s}_T$ of $\boldsymbol{s}(t)$. Consider their two trajectories $\boldsymbol{x}(t;t_0,\boldsymbol{x}_0)$ and $\boldsymbol{x}'(t;t_0,\boldsymbol{x}'_0)$ which are based on nearby initial conditions $\boldsymbol{x}_0,\boldsymbol{x}'_0$ whose $\boldsymbol{v}$ components belong to $\mathcal{B}$. Note that the $\boldsymbol{u}$ components of $\boldsymbol{x}(t;t_0,\boldsymbol{x}_0)$ and $\boldsymbol{x}'(t;t_0,\boldsymbol{x}'_0)$ become irrelevant after the first driving sample of $\boldsymbol{s}_T$ is applied. We shall consider the

asymptotic stability only of the $\boldsymbol{v}$ subsystem. The evolution of the difference $\Delta\boldsymbol{v}(t)=\boldsymbol{v}(t;t_0,\boldsymbol{x}_0)-\boldsymbol{v}'(t;t_0,\boldsymbol{x}_0')$ is governed by

$$\Delta\dot{\boldsymbol{v}}=\boldsymbol{F}_v(\boldsymbol{u},\boldsymbol{v})-\boldsymbol{F}_v(\boldsymbol{u}',\boldsymbol{v}')=\boldsymbol{D}_u\boldsymbol{F}_v(\boldsymbol{u},\boldsymbol{v})\Delta\boldsymbol{u}+\boldsymbol{D}_v\boldsymbol{F}_v(\boldsymbol{u},\boldsymbol{v})\Delta\boldsymbol{v}, \tag{7}$$

where $\boldsymbol{D}_u\boldsymbol{F}_v$ and $\boldsymbol{D}_v\boldsymbol{F}_v$ are the Jacobians of the vector field $\boldsymbol{F}_v$ with respect to the variables $\boldsymbol{u}$ and $\boldsymbol{v}$, respectively. All higher-order terms in Eq. (7) are neglected. The driving impulse at the moment t_n forces $\boldsymbol{u}$ and $\boldsymbol{u}'$ to the same new value $\boldsymbol{s}(t_n)$ and thus the difference $\Delta\boldsymbol{u}(t_n)$ to a new value $\boldsymbol{0}$. Thus, immediately after the moment t_n, $\boldsymbol{D}_u\boldsymbol{F}_v(\boldsymbol{u},\boldsymbol{v})\Delta\boldsymbol{u}$ can be neglected compared with $\boldsymbol{D}_v\boldsymbol{F}_v(\boldsymbol{u},\boldsymbol{v})\Delta\boldsymbol{v}$, and $\boldsymbol{u}$ can be replaced by $\boldsymbol{s}$.

(i) Consequently, Eq. (7) reduces to Eq. (6). (ii) If T is sufficiently small then $\boldsymbol{v}(t_n;t_0,\boldsymbol{x}_0)$, $\boldsymbol{v}'(t_n;t_0,\boldsymbol{x}_0')\in\mathcal{B}$ for all t_n or at least for a large portion of driving times t_n.

Properties (i) and (ii) along with the asymptotic stability of Eq. (5), assure that $\boldsymbol{v}(t;t_0,\boldsymbol{x}_0)$ and $\boldsymbol{v}'(t;t_0,\boldsymbol{x}_0')$ will approach each other immediately after the time point t_n. As time elapses from t_n, $\boldsymbol{v}(t;t_0,\boldsymbol{x}_0)$ and $\boldsymbol{v}'(t;t_0,\boldsymbol{x}_0')$ may begin to diverge due to the possibly unstable nature of Eq. (7). But, for sufficiently small T, the initial convergence after time t_n between $\boldsymbol{v}(t;t_0,\boldsymbol{x}_0)$ and $\boldsymbol{v}'(t;t_0,\boldsymbol{x}_0')$ dominates the overall behavior of $\Delta\boldsymbol{v}(t)$. As a consequence, $\lim_{t\to\infty}\Delta\boldsymbol{v}(t)=\boldsymbol{0}$. Since in addition $\Delta\boldsymbol{u}(t_n)=\boldsymbol{0}$ it follows that $\lim_{t\to\infty}\|\boldsymbol{x}(t;t_0,\boldsymbol{x}_0')-\boldsymbol{x}'(t;t_0,\boldsymbol{x}_0')\|=0$. Thus, Eq. (4) is asymptotically stable for sufficiently small driving periods T.

For large T values in Eq. (4), the trajectory $\boldsymbol{v}(t;t_0,\boldsymbol{x}_0)$ may one or more times leave and reenter $\mathcal{B}$ between two driving impulses by $\boldsymbol{s}_T$. Whether $\boldsymbol{v}(t_n;t_0,\boldsymbol{x}_0)$ belongs to $\mathcal{B}$ or not, depends on $\boldsymbol{v}(t_{n-1};t_0,\boldsymbol{x}_0)$, as well as on T. Thus, any change in T might exclude some points from $\mathcal{B}$ and include some new points in $\mathcal{B}$, which means that the region of asymptotic stability depends on T. A simple consequence of the Theorem is

Corollary. If Eq. (5) is unstable, then for sufficiently small driving periods T, the sporadically driven system (4) is unstable.

The validity of the Theorem is not conditioned on the asymptotic stability of the nondriven system

$$\dot{\boldsymbol{u}}=\boldsymbol{F}_u(\boldsymbol{u},\boldsymbol{v}),$$

$$\dot{\boldsymbol{v}}=\boldsymbol{F}_v(\boldsymbol{u},\boldsymbol{v}), \tag{8}$$

but when Eq. (8) is asymptotically stable then the Theorem is obvious and Eq. (4) is asymptotically stable for sufficiently large T. Therefore we pay attention only to the case when Eq. (8) is chaotic. In our examples we shall also consider the case when Eq. (8) is an unstable dynamical system in the sense that it diverges to infinity.

If Eq. (5) is asymptotically stable, then the Theorem implies the existence of a positive value T_H such that Eq. (4) is asymptotically stable for all $T<T_H$. The speed of the initial convergence (after time points t_n) of two trajectories of Eq. (4), starting at nearby initial conditions, is determined by the CLEs of Eq. (5). When $s(t)$ is generated by an identical dynamical system to Eq. (8) and is used in such a way as to synchronize Eq. (4) to the driving system, then the speed of the later chaotic divergence (in the intervals $t_n<t<t_{n+1}$) is determined by the positive Lyapunov exponent(s) (LE) of Eq. (8). Therefore, the critical value T_H is mainly determined by the CLEs of Eq. (5) and by the positive LE(s) of Eq. (8). If a driven dynamical system has many different asymptotically stable solutions, then their CLEs will be different, in general. Consequently, CLEs and T_H will be different for different asymptotically stable solutions of a sporadically driven system.

For the sporadically driven system (4) one can always find the stroboscopic map $\boldsymbol{M}_v:\mathcal{R}^N\to\mathcal{R}^{N-M}$ which is given by sampling the solution $\boldsymbol{x}(t;t_0,\boldsymbol{x}_0)$ at time points t_n

$$\boldsymbol{u}(n)=\boldsymbol{s}(n), \tag{9}$$

$$\boldsymbol{v}(n+1)=\boldsymbol{M}_v(\boldsymbol{v}(n),\boldsymbol{u}(n)), \tag{10}$$

where $\boldsymbol{s}(n)$, $\boldsymbol{u}(n)$, and $\boldsymbol{v}(n)$ denote $\boldsymbol{s}(t_n)$, $\boldsymbol{u}(t_n)$ and $\boldsymbol{v}(t_n)$, respectively. In Eq. (9) we use the fact that $\boldsymbol{u}(t_n)=\boldsymbol{s}(t_n)$. In this paper, we assume the uniqueness of solutions, that is, solutions of a dynamical system are uniquely determined by its defining differential equations and initial conditions. Thus, if in the limit $n\to\infty$ states of the sporadically driven dynamical system (4) at times t_n are determined by $\boldsymbol{s}(n)$ then it follows that even in the time intervals between two adjacent ''kicks'' by $\boldsymbol{s}(n)$ the dynamics of Eq. (4) is determined by $\boldsymbol{s}(n)$. In short, if and only if the driven map (9)–(10) is asymptotically stable with respect to $\boldsymbol{s}(n)$, then the sporadically driven dynamical system (4) is asymptotically stable with respect to $\boldsymbol{s}_T$. The numerical computation of the map $\boldsymbol{M}_v$ just by numerical integration of Eq. (4) over a certain period of time is always possible, but it does not simplify the question ''Is Eq. (4) asymptotically stable for a given T?'' When it is possible to analytically construct the map $\boldsymbol{M}_v$ then its analysis may be much simpler than the analysis of Eq. (4). This will be exploited in Sec. III where, due to the linearity of the driven systems, the construction of a stroboscopic map will be possible.

An example based on Chua's circuit illustrating the Theorem follows. A driving chain of one-dimensional impulses $s_T=x_{1T}=\{\ldots,x_1(-T),x_1(0),x_1(T),\ldots\}$ generated by Chua's circuit

$$\dot{\boldsymbol{x}}=\boldsymbol{C}(\boldsymbol{x}) \tag{11}$$

sporadically drives an identical copy of Chua's circuit

$$\dot{\boldsymbol{y}}=\boldsymbol{C}(\boldsymbol{y})+\left[\sum_{n=-\infty}^{+\infty}\delta(t-t_n)(x_1(t_n)-y_1(t_{n-}))\right],0,0\Big], \tag{12}$$

where the vector field $\boldsymbol{C}(\boldsymbol{x})$ is defined as $\boldsymbol{C}(\boldsymbol{x})=[\alpha(x_2-x_1-g(x_1)),x_1-x_2+x_3,-\beta x_2]$, $g(x)=m_1x+\frac{1}{2}(m_0-m_1)[|x+1|-|x-1|]$ and $m_0=-1.27,m_1=-0.68,\alpha=10.0,\beta=14.87$. In a large area around these parameter values Eq. (11) exhibits the chaotic double-scroll attractor.

In this example a one directional time discontinuous coupling between two time continuous dynamical systems (11) and (12) is performed. If Eq. (12) is asymptotically stable with respect to x_{1T} then Eq. (11) and Eq. (12) synchronize.

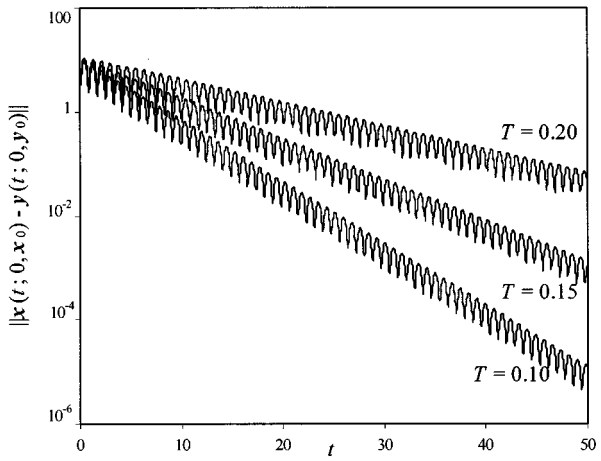

FIG. 1. Difference $\|\boldsymbol{x}(t;0,\boldsymbol{x}_0)-\boldsymbol{y}(t;0,\boldsymbol{y}_0)\|$ between two solutions of Eq. (11) and Eq. (12) which are based on two different initial conditions $\boldsymbol{x}_0$ and $\boldsymbol{y}_0$, for $T=0.10,0.15,0.20$.

The sum in Eq. (12) describes an infinite coupling between x_1 and y_1 only in the equidistant times t_n. As a result, $y_1(t)$ is forced to be equal to $x_1(t_n)$ at times t_n. Between two adjacent driving impulses, Chua's circuit (12) oscillates unforced and independently from the driving system (11). Denoting $\boldsymbol{v}=[y_2,y_3]$ and $\boldsymbol{u}=[y_1]$ one can readily see the compatibility of Eq. (12) with Eq. (4). The subsystem $\boldsymbol{v}=[y_2,y_3]$ is linear and its asymptotic stability can be easily proved: CLEs are $(-0.5,-0.5)$. Then from the Theorem it follows that there exists a maximal driving period T_H of the sequence of driving impulses that still allows Eq. (11) and Eq. (12) to synchronize. Numerically, we have found that the asymptotic stability of Eq. (12) is assured for $T<T_H=0.26$. This is illustrated in Fig. 1. Figure 1 shows the difference $\|\boldsymbol{x}(t;0,\boldsymbol{x}_0)-\boldsymbol{y}(t;0,\boldsymbol{y}_0)\|$ between two trajectories of Eqs. (11) and (12) which are based on two different initial conditions $\boldsymbol{x}_0$ and $\boldsymbol{y}_0$, for $T=0.10,0.15,0.20$.

The onset of synchronization between two identical dynamical systems which are sporadically coupled, as in Eqs. (11) and (12), can be viewed from another point of view. The driven dynamical system (12) nonlinearly interpolates the samples x_{1T} and produces the interpolated signal $y_1(t)$. If Eq. (12) is asymptotically stable for a given T, then the nonlinear interpolation is successful, that is, $y_1(t)=x_1(t)$. In this case, $x_1(t)$ is uniquely determined by its samples x_{1T}. The spectrum of the signal $\Sigma_{n=-\infty}^{+\infty}\delta(t-nT)x_1(nT)$ is periodic with period $\nu=1/T$ and is given by

$$X_1(f)\circ\left[\nu\sum_{n=-\infty}^{+\infty}\delta(f-n\nu)\right]=\nu\sum_{n=-\infty}^{+\infty}X_1(f-n\nu)$$

where $\circ$ denotes convolution. Due to the periodicity of its spectrum, the signal $\Sigma_{n=-\infty}^{+\infty}\delta(t-nT)x_1(nT)$ can be transmitted through an ideal low-pass channel with transfer function

$$H_{LP}(f)=\begin{cases}\dfrac{1}{\nu} & \text{for } |f|<\dfrac{\nu}{2}\\ 0 & \text{otherwise}\end{cases}$$

(the channel response to a single Dirac pulse excitation $\delta(t)$ is $[\sin(\pi\nu t)/\pi\nu t]$). Then the channel output may be written as

$$\widetilde{x}_1(t)=\frac{\sin(\pi\nu t)}{\pi\nu t}\circ\sum_{n=-\infty}^{+\infty}\delta(t-nT)x_1(nT)]$$

$$=\sum_{n=-\infty}^{+\infty}x_1(nT)\frac{\sin[\pi\nu(t-nT)]}{\pi\nu(t-nT)}.$$

The values of $\widetilde{x}_1(t)$ at the times nT are

$$\widetilde{x}_1(nT)=\sum_{m=-\infty}^{+\infty}x_1(mT)\frac{\sin(\pi(n-m))}{\pi(n-m)}=x_1(nT)$$

and the sequence x_{1T} can be exactly recovered by sampling $\widetilde{x}_1(t)$ at times nT, that is, $x_{1T}=\widetilde{x}_{1T}$. Then the sequence $\widetilde{x}_{1T}$ can be used to drive Eq. (12) and to successfully produce the interpolated signal $y_1(t)$. Thus, the concept of sporadic driving makes possible the synchronization of chaotic systems connected via bandlimited channels, and the transmission of chaotic signals through bandlimited channels. According to [17], power spectra of chaotic signals are exponentially decreasing and, therefore, with infinite width. But, as previously argued, despite the infinite width of their spectra, it is still possible to perfectly transmit chaotic signals through bandlimited channels using the concept of sporadic driving. This is not in contradiction to the well known sampling theorem [18], since the chaotic signals are generated (at least in this paper) by *deterministic* differential equations which, in addition, are *known* at the receiver. Only the initial conditions of the driving system are not known at the receiving end of the channel, i.e., at the interpolating side. On the contrary, the sampling theorem assumes no knowledge about the information source.

Even though the Theorem is of particular importance for the concept of sporadic driving, it does not address the following questions: (1) If a sporadically driven dynamical system is unstable for $T_0<T<T_0+\varepsilon$ where $\varepsilon>0$, does this imply that the system is necessarily unstable for all $T>T_0+\varepsilon$? (2) Do the CLEs (or at least the largest one) of a sporadically driven system monotonously rise as the driving period T increases? (3) If a time continuously driven system is unstable then is the sporadically driven version of the same system necessarily unstable for all T? One might expect that the natural answer to the previous questions is affirmative. For example, consider the first question. If for a driving period T_1 the chaotic behavior of the sporadically driven system overpowers the initial convergence of its trajectories immediately after the driving times t_n, then one may expect that this will also be the case for all $T>T_1$. As a little surprise we shall see that the answers to the three questions are all negative. The negative answer to the second question implies the existence of a driving period T with smallest CLEs of Eq. (4), and, therefore, the fastest convergence of nearby orbits and fastest synchronization. The answers will be given through examples exploiting sporadically driven linear systems. Certain phenomena will be encountered during these examples. Afterwards, we shall show that these phenomena also occur in the sporadically driven

Chua's circuit, the Lorenz system and the Rössler system. We shall also show that sporadic driving may result in *deadbeat synchronization in continuous-time systems* [19].

III. SPORADICALLY DRIVEN LINEAR SYSTEMS

In this section, we examine the asymptotic stability of sporadically driven linear systems. We use linear systems in our analysis since their analytical treatment is possible and the analytical construction of stroboscopic maps as in Eqs. (9) and (10) is feasible. We shall see several phenomena which are interesting and seem strange at first glance. Linearity of the driven system will enable us to explain the origins of these phenomena. Furthermore, the observed phenomena also appear when nonlinear systems are sporadically driven, as in Sec. IV.

Consider a linear two-dimensional system which is sporadically driven by an arbitrary signal $s(t)$, or more precisely by a sequence of samples s_T

$$\dot{x}_1 = ax_1 + bx_2 + \sum_{n=-\infty}^{+\infty} \delta(t-t_n)(s(t_n) - x_1(t_{n-})),$$

$$\dot{x}_2 = cx_1 + dx_2. \tag{13}$$

In order to examine the asymptotic stability of Eq. (13) we define a difference $\boldsymbol{e} = \boldsymbol{x} - \boldsymbol{x}'$ where the primed variables are from a system identical to Eq. (13) and driven by the same signal s_T. Due to the linearity of Eq. (13) it is easy to construct a stroboscopic map between two successive kicks by s_T

$$e_1(nT) = 0,$$

$$e_2((n+1)T) = \left[\sum_{i \neq k} \frac{d - p_k}{p_i - p_k} e^{p_i T} \right] e_2(nT) = r(T) e_2(nT), \tag{14}$$

where p_1 and p_2 are the eigenvalues of the matrix $\boldsymbol{A} = \left[\begin{smallmatrix} a & b \\ c & d \end{smallmatrix}\right]$. If $e_2(nT) \to 0$ when $n \to \infty$ then Eq. (13) is asymptotically stable. Therefore,

$$|r(T_H)| = \left| \frac{d - p_2}{p_1 - p_2} e^{p_1 T_H} + \frac{d - p_1}{p_2 - p_1} e^{p_2 T_H} \right| = 1 \tag{15}$$

determines T_H. LEs of the nondriven version of Eq. (13) are equal to the real parts of p_1 and p_2 while the CLE of $\boldsymbol{v} = [x_2]$ subsystem is equal to d. If p_1 and p_2 are real then T_H is completely determined through Eq. (15) by LEs p_1 and p_2 of the nondriven system and CLE d of the time continuously driven system. Otherwise, when p_1 and p_2 are complex conjugate, T_H in addition depends on their imaginary part.

The dependence of the ratio $r(T)$ on the driving period T is graphically presented in Figs. 2–4. If we choose a driving period T, such that $|r(T)| < 1$, then the system (13) is asymptotically stable, for $|r(T)| = 1$ it is stable, and otherwise it is unstable. For certain values of p_1 and p_2, interesting facts about the ratio $r(T)$ can be observed. Figure 2 shows the ratio $r(T)$ for different pairs of real eigenvalues p_1, p_2 when $d = -1.0 (< 0)$. First, we note that the subsystem $\boldsymbol{v} = [x_2]$ is asymptotically stable if and only if $d < 0$. According to the Theorem the asymptotic stability of the $\boldsymbol{v}$ subsystem implies the existence of positive T_H or, in other words, Eq. (15) has a positive solution for T_H. One can easily see this in another way. Immediately after the driving at the time $t = 0$ is applied, the difference $e_2(t)$ behaves as $\dot{e}_2 = de_2$ and initially the ratio $r(T)$ enters the region $(-1, 1)$. If the driving period is smaller than the value (if there is any) at which $r(T)$ leaves the region $(-1, 1)$ then Eq. (13) is asymptotically stable. Figure 2 illustrates several interesting cases: (a) Eq. (13) is asymptotically stable only in the initial region $T < T_H$ for $p_1 = 0.1, p_2 = -1.2$ (curve A) and $p_1 = 0.0001, p_2 = -0.2$ (curve D). (b) $T_H \to \infty$ when $p_1 = -0.1, p_2 = -1.2$ (curve B); (c) For $p_1 = -0.1, p_2 = -0.2$ (curve C) the region $T > T_H$ where Eq. (13) is unstable is followed by a region of T values where Eq. (13) is asymptotically stable.

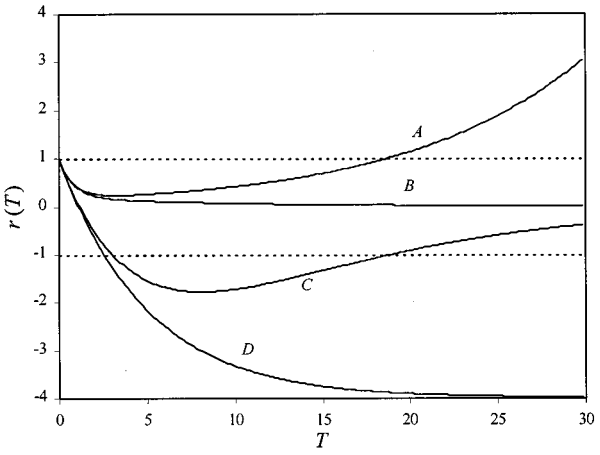

FIG. 2. The ratio $r(T)$ for different pairs of real eigenvalues p_1, p_2 when $d = -1.0$. $A - (p_1 = 0.1,\ p_2 = -1.2)$, $B - (p_1 = -0.1,\ p_2 = -1.2)$, $C - (p_1 = -0.1,\ p_2 = -0.2)$, $D - (p_1 = 0.0001,\ p_2 = -0.2)$.

Knowing the value $r(T)$, one can compute the largest CLE of Eq. (13) as $\lambda_1 = \ln|r(T)|$. Note that a smaller T does

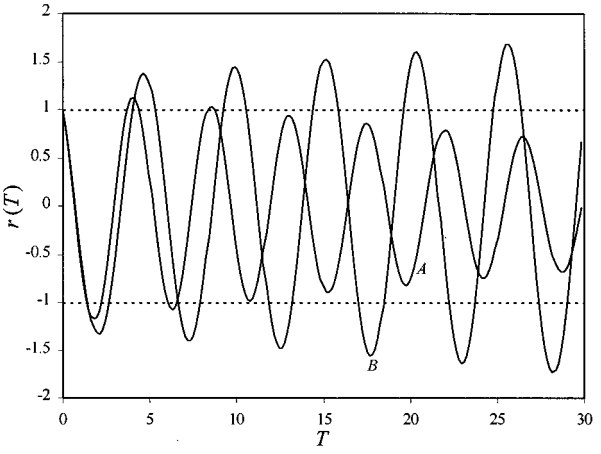

FIG. 3. The ratio $r(T)$ for different pairs of complex eigenvalues $p_1 = \rho + j\sigma, p_2 = \rho - j\sigma$, when $d = -1.0$. $A - (\rho = -0.02,\ \sigma = 1.4)$, $B - (\rho = 0.01,\ \sigma = 1.2)$.

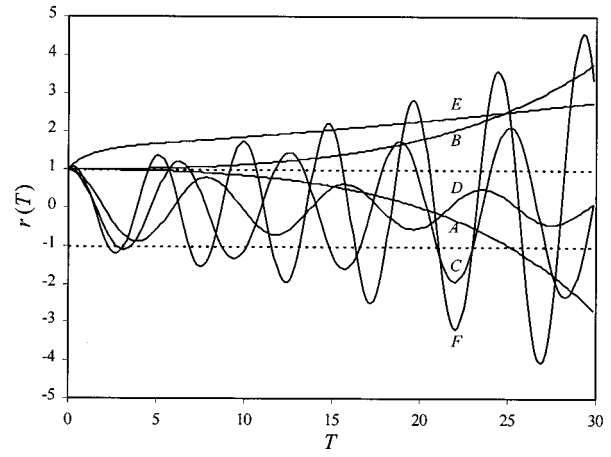

FIG. 4. Ratio $r(T)$ for different triples (d,p_1,p_2). $A-(d=0,\ p_1=0.1,\ p_2=0.02)$, $B-(d=0,\ p_1=0.1,\ p_2=-0.02)$, $C-(d=0,\ \rho=0.03,\ \sigma=1)$, $D-(d=0,\ \rho=-0.03,\ \sigma=0.8)$, $E-(d=0.5,\ p_1=0.02,\ p_2=-0.9)$, $F-(d=0.5,\ \rho=0.05,\ \sigma=1.3)$.

not mean higher stability and faster convergence during the synchronization transient. Furthermore, for certain pairs p_1,p_2 there exists a value $\hat{T}$, such that $r(\hat{T})=0$. If one chooses $T=\hat{T}$ then two copies of Eq. (13) driven by the same driving sequence s_T will synchronize after only two samples of s_T are received. This is similar to the notion of *dead-beat synchronization* of discrete-time systems [19].

Figure 3 shows the ratio $r(T)$ for different pairs of complex eigenvalues $p_1=\rho+j\sigma, p_2=\rho-j\sigma$ and $d<0$. When $\rho<0$ one or more regions of T values where Eq. (13) is unstable may occur. When $\rho>0$ infinitely many regions of T values where Eq. (13) is asymptotically stable occur, but their length decreases as T increases. One can choose arbitrarily large T which gives $|r(T)|<1$ and thus achieve synchronization.

What happens when d is not negative? According to the Corollary, if $d>0$ then $r(T)>1$ for sufficiently small T. In other words, if the time continuously driven subsystem $\boldsymbol{v}=[x_2]$ is unstable, then so is Eq. (13) for sufficiently small driving periods T. If $d=0$ then the time continuously driven subsystem $\boldsymbol{v}=[x_2]$ is stable and the behavior of $r(T)$ in the vicinity of $T=0$ is not obvious. On the basis of knowledge of only d, one cannot determine whether, for small T, stability will convert into instability or asymptotic stability. Figure 4 illustrates $r(T)$ for different triples $(d\geqslant 0,p_1,p_2)$. Surprisingly, even for $d\geqslant 0$ there may exist one or more regions of T values, where the sporadically driven system is asymptotically stable (curves A,C,D and F). Curve F shows that even for unstable time continuously driven subsystems one can sometimes *carefully* choose an arbitrarily large driving period T and achieve asymptotic stability. But one should be aware of the fact that the length of T regions where $|r(T)|<1$ decreases for larger T and therefore the driving period should be very accurately chosen. For certain dynamical systems, stability (curve B) and instability (curve E) at $T=0$ can turn into instability for all $T>0$.

Let us summarize the previous graphics and discussion. If $d<0$ $(d>0)$ then the subsystem $\boldsymbol{v}=[x_2]$ is asymptotically stable (unstable) and $T_H>0$ $(T_H=0)$ which is in accordance with the Theorem. If $d=0$, which means that Eq. (13) is stable for $T=0$, then whether this stability will convert into instability or asymptotic stability for $T>0$ depends on other entries of the matrix $\boldsymbol{A}$. If $d>0$ (Eq. (13) is unstable for $T=0$) then still there may exist infinitely many regions of T values where the sporadically driven system is asymptotically stable. Multiple regions of T values producing asymptotically stable sporadically driven system may also occur when $d\leqslant 0$.

This kind of dependence of the asymptotic stability of a sporadically driven system on T is not a special feature of linear systems. We have used the linear system (13) since its mathematical analysis is possible. Now we shall investigate the stability of sporadically driven nonlinear systems. The asymptotic stability of these systems will be analyzed through their CLEs, since their stability analysis through Lyapunov functions or linearized equations is much more difficult. Similar phenomena to those shown in Figs. 2–4 have been observed in these cases. When it occurs, we shall qualitatively explain the difference in the behavior of sporadically driven linear and nonlinear systems.

IV. SPORADICALLY DRIVEN NONLINEAR SYSTEMS

For the sake of simplicity, in this section, chaotic systems are sporadically driven by one-dimensional sequences produced by their nondriven counterparts. Therefore, the asymptotic stability of the driven system results in synchronized motion with the driving system. We have numerically investigated the dependence of the CLEs of the driven system on the driving period T, and have obtained similar dependencies to those for the linear system (13) which were given in Figs. 2–4. Several diagrams will be given which show these dependencies and indicate that the numerical results are in accordance with the Theorem. As is well known, a driven system is asymptotically stable if and only if its CLEs are all negative. CLEs of driven systems will be denoted as $\lambda_1\geqslant\lambda_2\geqslant\lambda_3$.

First we consider three sporadically driven Chua's circuits

$$\dot{\boldsymbol{y}}=\boldsymbol{C}(\boldsymbol{y})+\left[\sum_{n=-\infty}^{+\infty}\delta(t-t_n)(x_1(t_n)-y_1(t_{n-})),0,0\right], \tag{16}$$

$$\dot{\boldsymbol{y}}=\boldsymbol{C}(\boldsymbol{y})+\left[0,\sum_{n=-\infty}^{+\infty}\delta(t-t_n)(x_2(t_n)-y_2(t_{n-})),0\right], \tag{17}$$

$$\dot{\boldsymbol{y}}=\boldsymbol{C}(\boldsymbol{y})+\left[0,0,\sum_{n=-\infty}^{+\infty}\delta(t-t_n)(x_3(t_n)-y_3(t_{n-}))\right], \tag{18}$$

where the driving sequences x_{1T},x_{2T},x_{3T} are produced by Eq. (11). Figures 5–7 show the two largest CLEs of Eq. (16), Eq. (17), and Eq. (18), respectively. The third CLE for all three systems Eq. (16), Eq. (17), and Eq. (18) equals $-\infty$ and corresponds to the driven coordinate (see Appendix).

As stated in Sec. II, the subsystem $\boldsymbol{v}=[y_2,y_3]$ is asymptotically stable. CLEs λ_1 and λ_2 of Eq. (16) are negative for $T<0.26$, and almost identical to each other for $T<0.86$. For

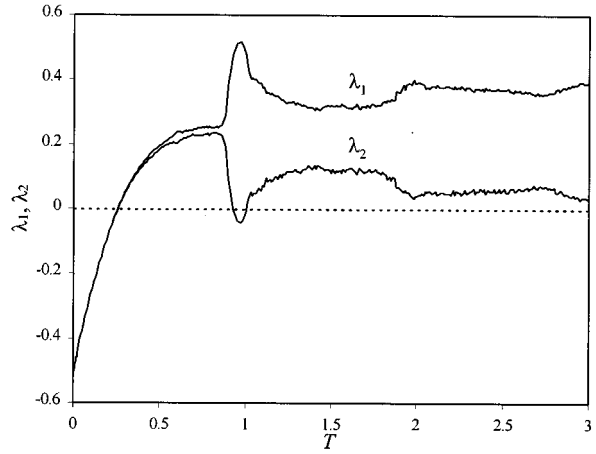

FIG. 5. Two largest CLEs of Chua's circuit (16) which is driven by x_{1T} generated by an identical Chua's circuit.

large T values, λ_1 tends to 0.39 and λ_2 tends to 0.0 which are just the two largest LEs of a nondriven Chua's circuit. This numerical observation can be generalized in the following way: CLEs of a sporadically driven system tend to the LEs of the nondriven system when $T \to \infty$.

The subsystem $\boldsymbol{v}=[y_1,y_3]$ is not asymptotically stable: its CLEs are 0.0 and -2.5. Due to the presence of a CLE with value 0.0, the Theorem does not determine whether Eq. (17) is asymptotically stable or not for small T. As shown on Fig. 6, numerical computations have indicated asymptotic stability of Eq. (17) for $T \in (0,0.83) \cup (1.25,1.49)$, while λ_1 achieves its minimum for $T=0.19$.

CLEs for $\boldsymbol{v}=[y_1,y_2]$ subsystem are 1.5 and -5.1. According to the Theorem, for sufficiently small values of the driving period T, the sporadically driven system (18) is unstable as can be seen in Fig. 7. Despite this, Eq. (18) is asymptotically stable for $T \in (0.4,0.85) \cup (1.56,1.68)$.

Also we have numerically examined the Lorenz system

$$\dot{\boldsymbol{x}}=\boldsymbol{L}(\boldsymbol{x}), \tag{19}$$

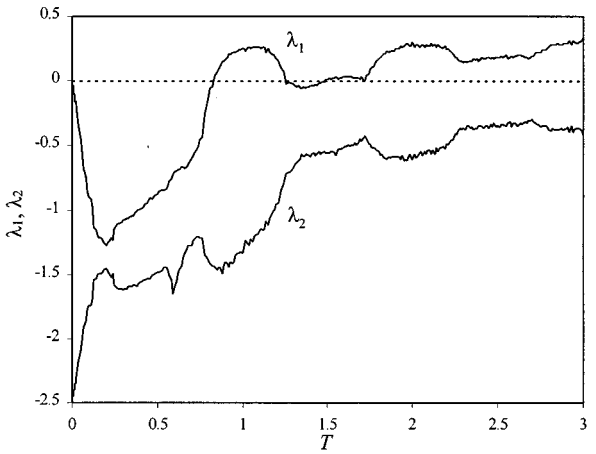

FIG. 6. Two largest CLEs of Chua's circuit (17) which is driven by x_{2T} generated by an identical Chua's circuit.

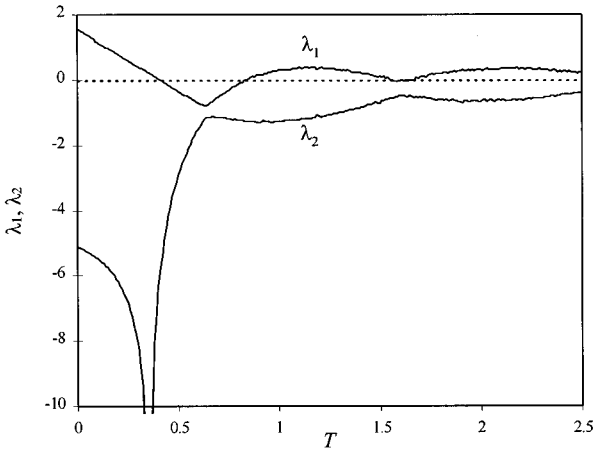

FIG. 7. Two largest CLEs of Chua's circuit (18) which is driven by x_{3T} generated by an identical Chua's circuit.

where $\boldsymbol{L}(\boldsymbol{x})=[16.0(x_2-x_1),45.6x_1-x_1x_3-x_2,x_1x_2-4.0x_3]$. Time sequences x_{1T},x_{2T},x_{3T} were used to sporadically drive three identical copies of Eq. (19)

$$\dot{\boldsymbol{y}}=\boldsymbol{L}(\boldsymbol{y})+\left[\sum_{n=-\infty}^{+\infty}\delta(t-t_n)(x_1(t_n)-y_1(t_{n-})),0,0\right], \tag{20}$$

$$\dot{\boldsymbol{y}}=\boldsymbol{L}(\boldsymbol{y})+\left[0,\sum_{n=-\infty}^{+\infty}\delta(t-t_n)(x_2(t_n)-y_2(t_{n-})),0\right], \tag{21}$$

$$\dot{\boldsymbol{y}}=\boldsymbol{L}(\boldsymbol{y})+\left[0,0,\sum_{n=-\infty}^{+\infty}\delta(t-t_n)(x_3(t_n)-y_3(t_{n-}))\right]. \tag{22}$$

Time continuously driven subsystems $\boldsymbol{v}=[y_2,y_3]$ and $\boldsymbol{v}=[y_1,y_3]$ are asymptotically stable and so are Eq. (20) and Eq. (21) for small T (see Figs. 8–10). The time continuously driven subsystem $\boldsymbol{v}=[y_1,y_2]$ is stable but is not asymptotically stable (its largest CLE is 0.0). Numerical integration of

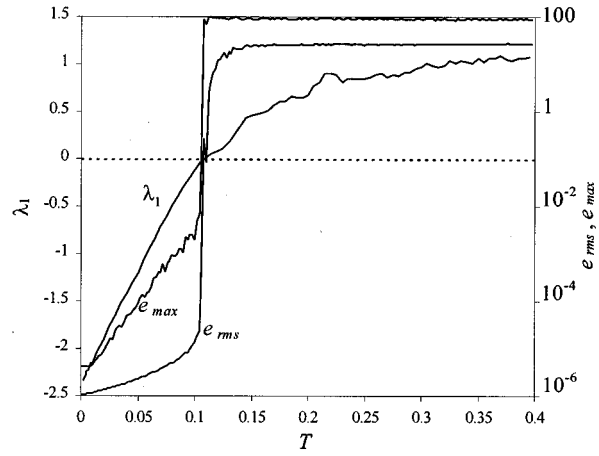

FIG. 8. Largest CLE, the average noise-induced synchronization error e_{rms}, and the maximal noise-induced synchronization error e_{max} for the Lorenz systems (20) which is driven by x_{1T} generated by an identical Lorenz system (19).

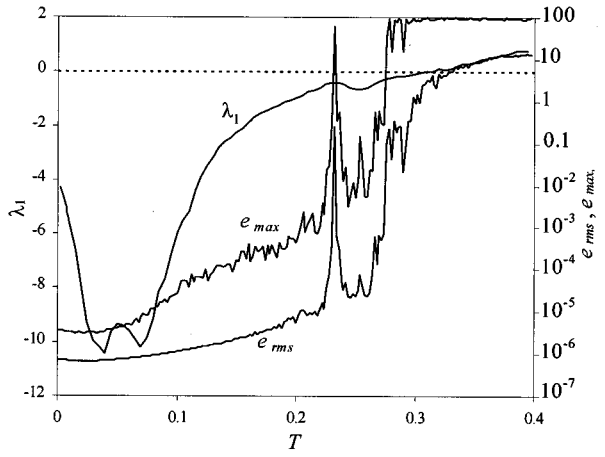

FIG. 9. Largest CLE, the average noise-induced synchronization error e_{rms}, and the maximal noise-induced synchronization error e_{max} for the Lorenz systems (21) which is driven by x_{2T} generated by an identical Lorenz system (19).

Eq. (22) showed that its stability for $T=0$ transforms into asymptotic stability for small $T>0$. Furthermore, Eq. (22) is asymptotically stable in three separated regions $T \in (0,0.02) \cup (0.07,0.12) \cup (0.27,0.31)$ (see Fig. 10). For all three systems (20), (21), and (22) we observed that λ_2 was much smaller than λ_1, and thus λ_2 is not shown in Figs. 8–10.

Numerical examinations over the Rössler system

$$\dot{\boldsymbol{x}} = \boldsymbol{R}(\boldsymbol{x}), \tag{23}$$

where $\boldsymbol{R}(\boldsymbol{x}) = [2.0 + x_1(x_2 - 4.0), -x_1 - x_3, x_2 + 0.45x_3]$, have also revealed nontrivial dependence between the CLEs of the sporadically driven systems

$$\dot{\boldsymbol{y}} = \boldsymbol{R}(\boldsymbol{y}) + \left[\sum_{n=-\infty}^{+\infty} \delta(t - t_n)(x_1(t_n) - y_1(t_{n-})), 0, 0 \right], \tag{24}$$

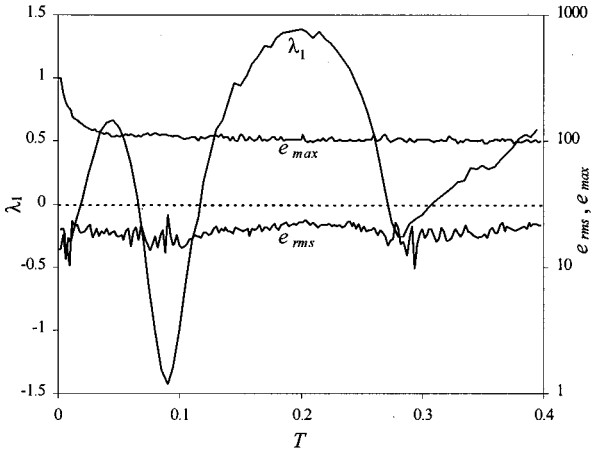

FIG. 10. Largest CLE, the average noise-induced synchronization error e_{rms}, and the maximal noise-induced synchronization error e_{max} for the Lorenz systems (22) which is driven by x_{3T} generated by an identical Lorenz system (19).

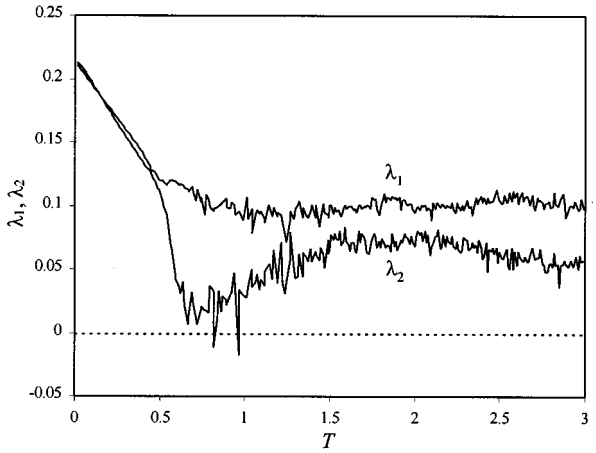

FIG. 11. Two largest CLEs of the Rössler system (24) which is driven by x_{1T} generated by an identical Rössler system.

$$\dot{\boldsymbol{y}} = \boldsymbol{R}(\boldsymbol{y}) + \left[0, \sum_{n=-\infty}^{+\infty} \delta(t - t_n)(x_2(t_n) - y_2(t_{n-})), 0 \right], \tag{25}$$

$$\dot{\boldsymbol{y}} = \boldsymbol{R}(\boldsymbol{y}) + \left[0, 0, \sum_{n=-\infty}^{+\infty} \delta(t - t_n)(x_3(t_n) - y_3(t_{n-})) \right] \tag{26}$$

and the driving period T. The time continuously driven subsystem $\boldsymbol{v} = [y_2, y_3]$ is unstable, and so is Eq. (24) for all driving periods (see Fig. 11). Furthermore, the two largest CLEs λ_1 and λ_2 of Eq. (24) are both positive. The subsystem $\boldsymbol{v} = [y_1, y_3]$ is also unstable, but Eq. (25) is asymptotically stable for $T \in (1.07, 2.74)$ (see Fig. 12). The subsystem $\boldsymbol{v} = [y_1, y_2]$ is asymptotically stable with $\lambda_1 = -0.23, \lambda_2 = -3.33$, and so is Eq. (26) for $T < 2.4$ (see Fig. 13). In the case of Eq. (25) and Eq. (26), there exists a driving period T which results in the smallest λ_1, and therefore fastest convergence of trajectories of the driven systems (25) and (26) to those of the driving system (23).

The dead-beat synchronization reported in Sec. III is possible mainly because the driven system is linear. As a result

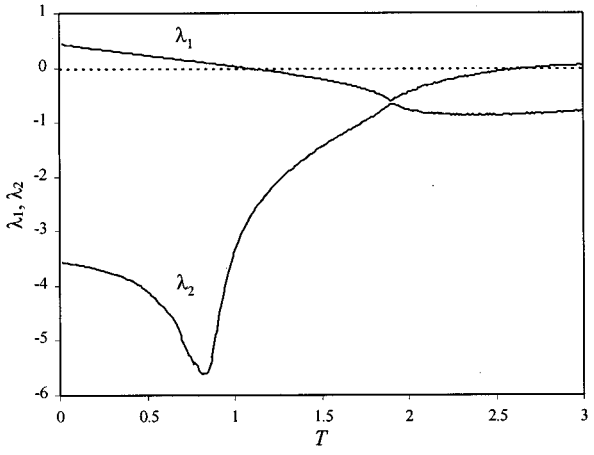

FIG. 12. Two largest CLEs of the Rössler system (25) which is driven by x_{2T} generated by an identical Rössler system.

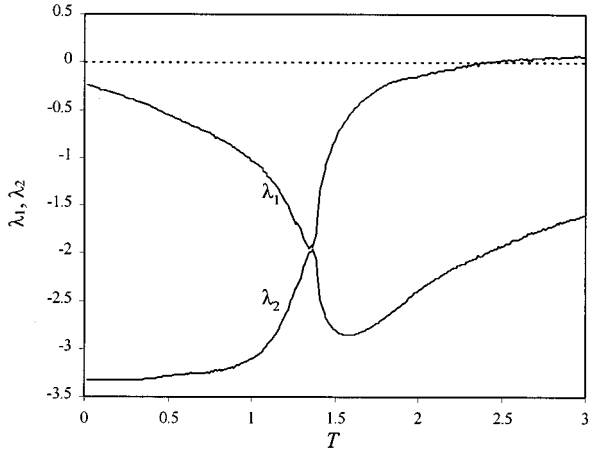

FIG. 13. Two largest CLEs of the Rössler system (26) which is driven by x_{3T} generated by an identical Rössler system.

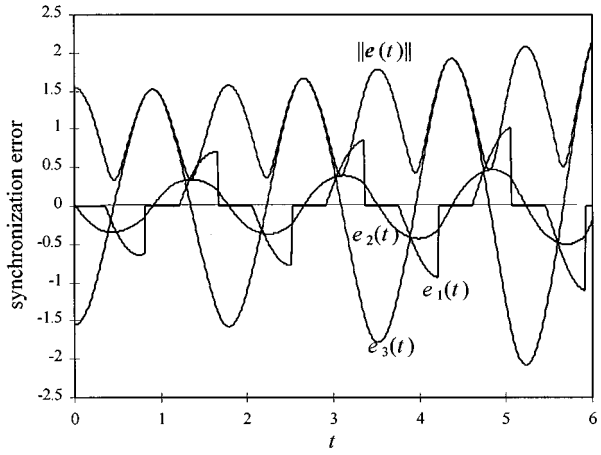

FIG. 15. Evolution of the differences $\|\boldsymbol{e}(t)\|$, $e_1(t)$, $e_2(t)$, and $e_3(t)$ for two Chua's circuits which are coupled via the method of sporadic driving with finite duration. $T=0.85$, $\tau=0.4$.

of the linearity, the solution(s) $\hat{T}$ of the equation $r(\hat{T})=0$ does not depend on the state of the driven system at the driving moment. Unlike the sporadic driving of linear systems, dead-beat synchronization was not achieved in the case of sporadically driven nonlinear systems. As can be easily observed from Figs. 5–13,16,17, the two largest CLEs of the examined sporadically driven nonlinear systems do not tend to $-\infty$ for any value of the driving period T. Whether dead-beat synchronization in sporadically driven nonlinear systems is possible and under what conditions is the subject of our current research.

V. GENERALIZATION OF SPORADIC DRIVING

A. Combination with other synchronization methods

Several generalizations of Pecora-Carroll (PC) synchronization method have been proposed so far. The PC method relies on decompositions of the vector field into two parts: drive and response, where each part corresponds to a subspace spanned by the originally chosen coordinates. For every vector field the number of PC decompositions is limited. Furthermore, not all of the decompositions result in an asymptotically stable response subsystem. In [3,5], it was proposed that dynamical systems should be seen as objects whose coordinates can be chosen by the observer and are not given *a priori*. On this basis, a more general drive-response decomposition (active-passive decomposition (APD) in terms of [3,5]) was proposed. Neither the drive (active) nor the response (passive) part needs to correspond to a subspace spanned by the originally chosen coordinates. As a result, the number of APD decompositions is infinite, and one can hopefully find an APD decomposition which is better than all PC decompositions in the sense that the CLEs of the driven system are more negative and it responds better to the driving system. It is rather straightforward to generalize sporadic driving in this direction. Actually, a sporadically driven APD decomposition is also described by Eq. (4), with the only difference being that $\boldsymbol{u}$ and $\boldsymbol{v}$ are the new coordinates obtained through a change of the old coordinates $\boldsymbol{x}$, and $\boldsymbol{F}_u$ and $\boldsymbol{F}_v$ are a decomposition of the original vector field $\boldsymbol{F}$ and correspond to the new coordinates $\boldsymbol{u}$ and $\boldsymbol{v}$. The Theorem is also valid for sporadically driven APD decompositions. If the APD decomposition is carefully chosen, then the CLEs of the continuously driven passive subsystem may be very negative. Thus, the sporadically driven APD decomposition can achieve asymptotic stability for large values of T, and the sequence $\boldsymbol{s}_T$ can be transmitted through a channel with narrow band.

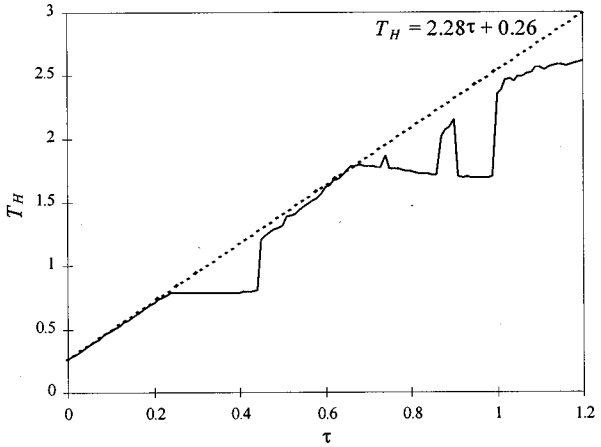

FIG. 14. Dependence of the maximum value of the driving period T_H that still yields synchronized motion between two Chua's circuits on the driving duration τ. The Chua's circuits are coupled via the method of sporadic driving with finite duration.

Sporadic driving can also be generalized in the way the Fujisaka-Yamada method [20] generalizes Pecora-Carroll driving. The following driven dynamical system:

$$\dot{\boldsymbol{u}}=\boldsymbol{F}_u(\boldsymbol{u},\boldsymbol{v})+\sum_{n=-\infty}^{+\infty}\delta(t-t_n)\boldsymbol{E}(\boldsymbol{s}(t_n)-\boldsymbol{u}(t_{n-}))$$

$$\dot{\boldsymbol{v}}=\boldsymbol{F}_v(\boldsymbol{u},\boldsymbol{v}) \tag{27}$$

behaves independently from the driving signal $\boldsymbol{s}_T$ except for the times t_n when the $\boldsymbol{u}$ components are forced to new values

$\boldsymbol{u}(t_n)=(\boldsymbol{I}-\boldsymbol{E})\boldsymbol{u}(t_{n-})+\boldsymbol{E}\boldsymbol{s}(t_n)$, where $\boldsymbol{E}$ is the coupling matrix, and $\boldsymbol{I}$ is an identity matrix. Equation (27) reduces to Eq. (4) when $\boldsymbol{E}=\boldsymbol{I}$.

One may also apply sporadic driving to two-directionally coupled systems: $\dot{\boldsymbol{x}}=\boldsymbol{F}(\boldsymbol{x})+\Sigma_{n=-\infty}^{+\infty}\delta(t-t_n)\boldsymbol{E}(\boldsymbol{x}'(t_n)-\boldsymbol{x}(t_{n-}))$ and $\dot{\boldsymbol{x}}'=\boldsymbol{F}(\boldsymbol{x}')+\Sigma_{n=-\infty}^{+\infty}\delta(t-t_n)\boldsymbol{E}'(\boldsymbol{x}(t_n)-\boldsymbol{x}'(t_{n-}))$, where $\boldsymbol{E}$ and $\boldsymbol{E}'$ denote the coupling matrices.

B. Sporadic driving with finite duration

In practical realizations of sporadic driving with electronic circuits, the driving duration around times t_n will always be finite and nonzero. This is our motivation for generalizing the idea of sporadic driving in the following way. The driving is again applied periodically, but its duration is finite rather then tending to zero. The duration of the driving is denoted as τ. Each driving period is divided into two parts with lengths τ and $T-\tau$. At the beginning of each driving period, during the time interval τ, the response system is being driven by the driving signal as

$$\boldsymbol{u}=\boldsymbol{s}(t),$$

$$\dot{\boldsymbol{v}}=\boldsymbol{F}_v(\boldsymbol{u},\boldsymbol{v}), \tag{28}$$

while in the remaining time interval, with length $T-\tau$, the driven system behaves independently from the driving signal

$$\dot{\boldsymbol{u}}=\boldsymbol{F}_u(\boldsymbol{u},\boldsymbol{v}),$$

$$\dot{\boldsymbol{v}}=\boldsymbol{F}_v(\boldsymbol{u},\boldsymbol{v}). \tag{29}$$

We illustrate the concept of sporadic driving with finite duration through an example with two identical Chua's circuits which are coupled in their first coordinates x_1 and y_1. The driven Chua's circuit behaves independently and chaotically only during the time periods with length $T-\tau$ which occur periodically with period T. During the periodic time intervals with length τ the y_1 component of the driven Chua's circuit is being kept equal to the component x_1 of the driving Chua's circuit.

Figure 14 shows the functional relation between the driving duration τ and the maximum value of the driving period T_H that still allows synchronized motion between the two Chua's circuits. Surprisingly, T_H versus τ is not a monotonously increasing function as one would intuitively expect. In certain τ ranges, an increase in the driving duration does not contribute to any increase in T_H. In the remaining τ ranges the dependence between τ and T_H is approximately linear. In order to clarify this surprising dependence we give the following analysis.

During the intervals with length τ, CLEs of Eq. (28) are in power and for Chua's circuit they are both -0.5. In the remaining intervals each with length $T-\tau$ Chua's circuit (29) behaves freely and its positive LE is 0.39. Convergence during τ and divergence during $T-\tau$ cancel each other when $-0.5\tau+0.39(T-\tau)=0$, that is, $T=2.28\tau$. When $\tau=0$ Chua's circuit (29) is asymptotically stable even for positive T, i.e., for $T<0.26$, since y_1 component of the driven system is made equal to the component x_1 of the driving system at times t_n. So, we linearly approximate the dependence between T_H and τ as $T_H=0.26+2.28\tau$ (dotted curve at Fig. 14).

In the driving intervals with length τ, the difference $\boldsymbol{e}=\boldsymbol{x}-\boldsymbol{y}$ evolves according to

$$\begin{bmatrix}\dot{e}_2\\ \dot{e}_3\end{bmatrix}=\begin{bmatrix}-1 & 1\\ -\beta & 0\end{bmatrix}\times\begin{bmatrix}e_2\\ e_3\end{bmatrix}, \tag{30}$$

while $e_1=0$. One can solve Eq. (30) and see that $e_2(t)$ and $e_3(t)$ approach 0 in an oscillating manner. Therefore, larger driving duration τ does not mean smaller difference $\|\boldsymbol{e}(\tau)\|$ for every $\boldsymbol{e}(0)$, and it might also mean larger projection of $\boldsymbol{e}(\tau)$ on the unstable eigenspace. During the nondriving intervals the driven Chua's circuit behaves chaotically and $e_2(t)$ and $e_3(t)$ diverge from 0 in an *oscillating* manner. The difference $\boldsymbol{e}(T)$ achieved at the end of the nondriving interval depends not only on the LEs of the driving Chua's circuit, but also on $\|\boldsymbol{e}(\tau)\|$ and the projections of $\boldsymbol{e}(\tau)$ on the unstable and stable eigenspaces. Figure 15 shows $\|\boldsymbol{e}(t)\|$, $e_1(t)$, $e_2(t)$, and $e_3(t)$ for $T=0.85$ and $\tau=0.4$.

As a result of the oscillatory behavior around 0 of $e_2(t)$ and $e_3(t)$ during both driving and nondriving intervals, for certain ranges of τ values $[\tau\in(0.24,0.44)\cup(0.66,0.86)\cup(0.91,0.99)]$ larger driving interval τ allows smaller maximum value of the nondriving interval $T_H-\tau$ and does not contribute to any increase in T_H (see Fig. 14).

VI. SPORADIC DRIVING IN PRESENCE OF NOISE

In this section we address the sensitivity of the synchronized motion of sporadically coupled identical chaotic systems to noise influence. It is a well known fact that the CLEs are a necessary and sufficient condition for synchronized motion [1,2]. From their definition it is obvious that they, as well as the LEs, refer only to the long-term behavior. However, when all the CLEs are negative there can still exist points in the synchronization manifold $\boldsymbol{x}=\boldsymbol{y}$ whose maximal LE for perturbations transverse to the synchronization manifold is positive when computed over a *finite* time interval [21]. Such fluctuations in the CLEs computed over a finite time are the reason that the synchronization transient is not accompanied with a monotonous approach towards the synchronization manifold, but instead brief intermittent high-magnitude (comparable to the size of the attractor) departures from the synchronization manifold appear.

In the real systems the noise is inevitably present. Therefore we are interested only in a synchronized motion which is resistant to the negative influence of noise, i.e., in a high-quality synchronized motion in the language of [22,23]. The noise permanently disturbs the synchronized motion which gives rise to a sustained transient behavior. Since the CLEs do not characterize the transient behavior they cannot be successfully exploited to quantitatively express the noise influence, and their negativity is not a sufficient condition for the high-quality synchronized motion. As shown in [22,23] the synchronized motion in the real chaotic systems may be interrupted with outbreaks of desynchronized bursty behavior provoked by the noise. The main cause of the desynchronized bursts are the phase points lying in the synchronization

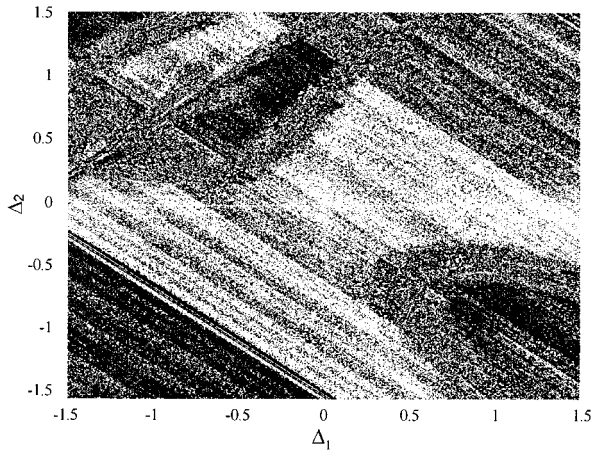

FIG. 16. A 600×600 grid of the riddled basin of attraction for Eqs. (19) and (22) when $T=0.28$. The phase points $[p_1+\Delta_1,p_2+\Delta_2,p_3,p_1+\Delta_1,p_2-\Delta_2,p_3]$ that go to the in-phase manifold are represented as white dots, while the black dots correspond to the initial states going to the in-antiphase manifold. $p_1=0.5085, p_2=1.0552, p_3=24.1274$.

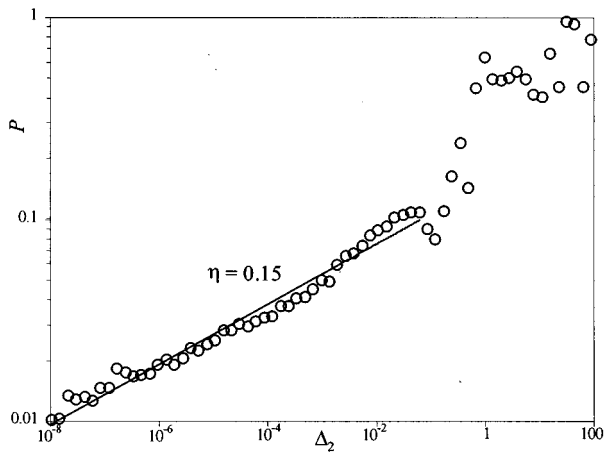

FIG. 17. The probability P of going to the in-antiphase manifold as function of the transverse deviation Δ_2. $T=0.28$.

manifold that have one or more positive CLEs computed over a finite time, that is, as pictorially expressed in [22,23], the unstable invariant sets embedded within the chaotic attractor and therefore lying in the synchronization manifold whose maximal CLE is positive. The invariant sets of this kind are unstable both to perturbations lying in the synchronization manifold and being transverse to it. When the states of the coupled systems come close to such an invariant set, the disturbance in the synchronized motion caused by the noise gets amplified by the transverse instability of the invariant set provoking the motion to be kicked off the synchronization manifold. Obviously, the proper criterion for a high-quality synchronization is the negativity of the CLEs of all the invariant sets embedded within the chaotic attractor [22,23]. Although this criterion sounds very simple and mathematically precise it is rather impractical and cumbersome due to the infinite number of the invariant sets whose transverse stability must be checked. In [23] it was proposed to exploit the negativity of the time derivative of Lyapunov functions as a tool to show that the perturbations caused by the noise decay permanently rather than sometimes being amplified by the transversely unstable invariant sets. But, finding a Lyapunov function which proves the decay of the noise-induced perturbations is a very difficult task. A recent work [24] has eased the checking of the transverse stability of the invariant sets by pointing out that typically the periodic orbits with low period are the invariant sets with largest CLE. Identifying the transverse stability of the low-period orbits may explain the reasons for the existence or nonexistence of the high quality synchronization. Still the direct measurement (when possible) of the noise-provoked disturbances to the synchronized motion is the most reliable and the easiest tool to directly determine the quality of the synchronization. If the synchronized motion of two coupled systems in the presence of noise is not interrupted by high-magnitude desynchronized burst for a long time (during which the coupled systems come very close to every point on the chaotic attractor) then we can safely conclude that the synchronization is of high quality.

What are the consequences for quality of the synchronization in a noisy environment when the chaotic systems are sporadically coupled? Two sporadically coupled chaotic systems, in the time intervals when oscillating independently from each other, amplify the noise perturbation due to their chaotic nature and the permanent decrease in their synchronization error is not possible. Thus, from the point of view of the sporadic driving the negativity of the time-derivative of the Lyapunov functions is an inapplicable tool. In the case of time-discontinuous couplings the maximal CLE for a given initial state which is computed over a finite time depends also on the time of appearance of the next driving impulse. We have seen in Sec. IV that the CLEs for coupled chaotic systems may depend on the driving period T in a very complicated manner. It is reasonable to assume that the maximal CLE for an unstable periodic orbit lying in the synchronization manifold may depend on the driving period also in a complicated way (the driving is done by the unstable periodic orbit generated by another dynamical system [22]). So, while the chaotic attractor gets more negative maximal CLE with increase in T, an unstable periodic orbit may experience more positive maximal CLE. On the contrary, a change in T may turn the otherwise positive maximal CLE of an unstable invariant set into a negative one, that is, a high quality synchronized motion may emerge when sporadic driving is used instead of a time continuous driving.

Such a complication of the issue of noise influence in the case of sporadic driving has strengthened our decision to express the quality of the synchronized motion of sporadically coupled systems through a direct measurement of the synchronization error. Here we present results from numerical experiments concerning the quality of synchronized motion of the sporadically coupled Lorenz systems (19)–(22) in the presence of small additive noise. We used the fourth-order Runge-Kutta method. In real systems, both the driving and the driven system, as well as the driving signal during its transmission, are contaminated by the noise. Thus we added small random noise to all the coordinates of the driving and the driven systems, and to the driving signal. The random noise had uniformly distributed amplitudes in the range

$(-10^{-7},+10^{-7})$. The adjacent noise samples were uncorrelated, and so were the noises added to any two different coordinates.

After the initial time period of length 10, which was allowed for the transient oscillations to die out, we measured the synchronization error $e(t)=\|\boldsymbol{x}(t)-\boldsymbol{y}(t)\|$. Figures 8–10 present the dependence of e_{rms} and e_{max} on the driving interval T, where e_{rms} denotes the average value of $e(t)$ averaged over a time interval of length 12000, and e_{max} denotes the maximal value of the error $e(t)$ observed during the same time. Since e_{rms} is averaged over the whole chaotic attractor it is no surprise that in Figs. 8 and 9 it follows the changes in the largest CLE [23,25,26]. The maximal error e_{max}, which is sensitive to the local instabilities of the synchronized motion, reveals the magnitudes of the possible intermittent bursts, and values of e_{max} small compared to the attractor size are a clear indication of a high-quality synchronized motion. As shown in Figs. 8 and 9 the T regions of high-quality synchronization for the pairs of Lorenz systems (19) and (20), and (19) and (21) agree very well with the T regions of asymptotic stability. Highering and lowering the noise level did not cause any qualitative change to the noise sensitivity except for the scaling of e_{rms} and e_{max} proportional to the change in the noise level. These results, along with the simulations we carried out for the Chua's circuit and the Rössler system, clearly indicate that a high-quality synchronized motion between sporadically coupled chaotic systems is possible. Furthermore, high-quality synchronization also emerged in the cases when the time continuous driving does not lead to synchronized motion at all (for example, driving the Chua's circuit with x_{2T} or x_{3T} or driving the Rössler system with x_{3T}).

According to Fig. 10, a high-quality synchronization of two Lorenz systems when driving with x_{3T} is not achievable for any driving period T despite the negativity of the largest CLE in three separate T regions. Here we show that the underlying reason is the riddled basin of the chaotic attractor lying in the synchronization manifold. A chaotic attractor may have a riddled basin only if it lies in an invariant manifold with lower dimension than that of the full space and another attractor exists outside the manifold [28]. This condition is fulfilled in the case of synchronized identical chaotic systems where the motion settles in the manifold $\boldsymbol{x}=\boldsymbol{y}$, whose dimension is 1/2 of the dimension of the full space. Riddling of the basin means that arbitrarily close to the points that belong to the basin of the chaotic attractor one can find points with a nonzero measure that go to the other attractor. Even for the points that are arbitrarily close to the invariant manifold there is a nonzero probability that they will eventually settle on the other attractor. When a noise is present the chaotic oscillations are permanently being moved off the invariant manifold. The noise repeatedly moves the chaotic state to the basin of the other attractor and eventually the motion will settle on the other attractor.

In the dynamics of the Lorenz system there is a symmetry $(x_1,x_2)\rightarrow(-x_1,-x_2)$. Due to this symmetry the two Lorenz systems (19) and (22) can synchronize either in-phase $y_1=x_1$, $y_2=x_2$, $y_3=x_3$ or in-antiphase $y_1=-x_1$, $y_2=-x_2$, $y_3=x_3$, and, furthermore, the two synchronized states (in-phase and in-antiphase) have identical CLEs and they gain and lose their stability [27] simultaneously as T changes. Our numerical simulations have shown that both chaotic attractors (one lying in the manifold $y_1=x_1$, $y_2=x_2$,$y_3=x_3$, and the other lying in the manifold $y_1=-x_1$, $y_2=-x_2$, $y_3=-x_3$) have riddled basins of attraction for *all* driving periods T where the largest CLE is negative. In terms of [28] the two basins are called intermingled. Figure 16 shows a two-dimensional slice of the basin of attraction of the in-phase and in-antiphase attractors. We have randomly chosen a point $[p_1,p_2,p_3]$ lying on the Lorenz chaotic attractor. Numerically solving Eqs. (19) and (22) (without adding noise) we have determined the basin to whom a phase point $[p_1+\Delta_1,p_2+\Delta_2,p_3,p_1+\Delta_1,p_2-\Delta_2,p_3]$ belongs where $[p_1+\Delta_1,p_2+\Delta_2,p_3]$ and $[p_1+\Delta_1,p_2-\Delta_2,p_3]$ are the states at $t=0$ of Eq. (19) and Eq. (22), respectively, Δ_1 is the deviation along the in-phase manifold $\boldsymbol{x}=\boldsymbol{y}$ and Δ_2 is the deviation transverse to the same manifold. We have also magnified different regions of Fig. 16 and have inspected basins near other points $[p_1',p_2',p_3']$. The riddled structure of Fig. 16 was always present. As previously said, for riddled basins even arbitrarily close points to the manifold $\boldsymbol{x}=\boldsymbol{y}$ have nonzero probability of settling to the in-antiphase manifold. So, another proof of the presence of a riddled basin in Eqs. (19) and (22) is Fig. 17, where P denotes the numerically estimated probability that a randomly chosen point with transverse deviation Δ_2 belongs to the basin of the chaotic attractor lying in the in-antiphase manifold. The probability P scales as a power law with Δ_2, i.e., $P\sim\Delta_2^{\eta}$ which is in accordance with the theoretical results in [28]. Due to the riddled basins neither in-phase nor in-antiphase synchronization can persist indefinitely in presence of noise, and the Lorenz systems (19) and (22) repeatedly switch from in-phase to in-antiphase synchronization and vice versa. The time intervals with in-antiphase synchronization are responsible for the large values of the errors e_{rms} and e_{max}.

VII. TESTING EXPERIMENTAL MODELS WITH SPORADIC DRIVING

The problem of determination of equations of motion of a chaotic system on basis of experimentally collected data is rather interesting and useful. Most often, experimental measurements produce scalar data $z_L=\{z(0),z(L),\ldots,z(N_zL)\}$ where L denotes the sampling interval. Then, z_L is used to construct a sequence of phase-space vectors $\boldsymbol{s}_L=\{\boldsymbol{s}(0),\boldsymbol{s}(L),\ldots,\boldsymbol{s}(NL)\}$. Here we shall not be concerned with the phase-space reconstruction method and shall assume that $\boldsymbol{s}_L$ is already given. The main objective in nonlinear time-series modelling is to find a vector field $\boldsymbol{F}$ (or a map $\boldsymbol{M}$) which is optimal according to a certain criterion and models the real system with differential equations

$$\dot{\boldsymbol{x}}=\boldsymbol{F}(\boldsymbol{x}). \tag{31}$$

Having chosen the optimal vector field $\boldsymbol{F}$, synchronization can be used to test how precisely $\boldsymbol{F}$ models the equations of motion [29]. As proposed in [29], linear coupling should be used for that purpose

$$\dot{\boldsymbol{x}}=\boldsymbol{F}(\boldsymbol{x})+\boldsymbol{E}(\hat{\boldsymbol{s}}(t)-\boldsymbol{x}), \tag{32}$$

where $\hat{\boldsymbol{s}}(t)$ denotes the linear interpolation of the sequence $\boldsymbol{s}_L$, and the coupling matrix $\boldsymbol{E}$ may have only one nonzero element $E_{ii}=\mu$ that belongs to the main diagonal. Since the signal $\boldsymbol{s}(t)$ is known only at discrete times, a linear interpolation is used to compute $\boldsymbol{s}(t)$ at other points of the time scale which produces the linearly interpolated signal $\hat{\boldsymbol{s}}(t)$. The synchronization test for the validity of the modelling vector field $\boldsymbol{F}$ relies on two solutions $\boldsymbol{x}(t)$ and $\boldsymbol{x}'(t)$ of Eq. (32). Both solutions start at $\boldsymbol{s}(0)$, but $\boldsymbol{x}(t)$ is obtained for $\mu>0$, and $\boldsymbol{x}'(t)$ for $\mu=0$. If the driving coordinate x_i and the coupling strength μ are properly chosen and assure asymptotic stability of Eq. (32), and $\boldsymbol{F}$ is structurally close to the true vector field then the sequence $\boldsymbol{x}_L$ should be close to the experimentally obtained sequence $\boldsymbol{s}_L$. On the contrary, the chaotic instability of Eq. (32) when $\mu=0$ causes $\boldsymbol{x}'_L$ to diverge from $\boldsymbol{s}_L$. Thus, if the mean difference $D=\overline{\|\boldsymbol{x}_L-\boldsymbol{s}_L\|}$ is much smaller then $D'=\overline{\|\boldsymbol{x}'_L-\boldsymbol{s}_L\|}$, then it should be accepted as a good proof that $\boldsymbol{F}$ is a good model for the real chaotic system. However, even when $\boldsymbol{F}$ perfectly models the real chaotic system, $\boldsymbol{x}(t)$ does not tend to $\hat{\boldsymbol{s}}(t)$, and $\boldsymbol{x}_L$ does not tend to $\boldsymbol{s}_L$, since $\hat{\boldsymbol{s}}(t)$ is not a true solution of Eq. (31). Thus D is not equal to 0 which decreases the gap between D and D'. Having in mind that sporadically coupled chaotic systems may express asymptotic stability, we propose that in the synchronization test Eq. (32) one should use sporadic driving instead of the time continuous driving

$$\dot{\boldsymbol{x}}=\boldsymbol{F}(\boldsymbol{x})+\sum_{n=-\infty}^{+\infty}\delta(t-t_n)\boldsymbol{E}(\boldsymbol{s}(t_n)-\boldsymbol{x}(t_{n-})), \tag{33}$$

where T could be any multiple of L. If the sampling interval L is sufficiently small [if it is not then also the synchronization test employing Eq. (32) will not work] then one can find a pair of values for parameters T and μ such that Eq. (33) is asymptotically stable. The synchronization test employing Eq. (33) will give smaller D compared to the case when it exploits Eq. (32) and consequently a bigger margin to D'.

Furthermore, as it was shown in Sec. II, the sporadically driven model (33) produces a time continuous signal $\boldsymbol{x}(t)$ and nonlinearly interpolates the experimental data z_L if the modelling vector field is perfect.

In some cases experimental measurements are not equidistant in time. Still our modified synchronization test of experimental models is applicable. Sporadic driving is not restricted only to time-equidistant driving, and asymptotic stability of a time discontinuously driven system can also be achieved when the driving impulses appear nonequidistantly in time according to a certain deterministic rule or the time interval between the driving impulses is a random variable. So, in the case of nonequidistant data the time discontinuous driving of the experimental model should follow the same rule as the process of measurement. An exception to this rule may appear when the measurements are done too often, in which case not every vector in the sequence of reconstructed phase-space vector is necessary to obtain asymptotically stable experimental model.

VIII. CONCLUSION

We have numerically and analytically examined the sporadic driving of time continuous systems. The dependence of the asymptotic stability of sporadically driven *linear* systems on the driving period is analytically investigated. Similar dependence has been numerically observed in the case of sporadically driven *nonlinear* systems such as Chua's circuit, Lorenz, and Rössler system. Generalization of sporadic driving in the direction of active-passive decomposition, linear one- and two-directional coupling, and finite duration of the driving have been proposed. Nontrivial dependence of the maximal driving period T_H which still yields asymptotic stability of the driven system on the driving duration τ has been reported and explained. Our numerical experiments on the influence of noise on the synchronized motion have shown that high-quality synchronization between sporadically coupled systems is possible. High-quality synchronization is possible even in some cases where synchronization cannot be achieved with continuous coupling. On the basis of sporadic driving, the synchronization test [29] for the validity of models derived from experimental data has been modified. The results of the modified test are more reliable.

APPENDIX

Lemma. The k smallest conditional Lyapunov exponents of a continuous system (A1) that is sporadically driven by a k-dimensional sequence $\boldsymbol{s}_T$

$$\dot{\boldsymbol{u}}=\boldsymbol{F}_u(\boldsymbol{u},\boldsymbol{v})+\sum_{n=-\infty}^{+\infty}\delta(t-t_n)(\boldsymbol{s}(t_n)-\boldsymbol{u}(t_{n-}))$$

$$\dot{\boldsymbol{v}}=\boldsymbol{F}_v(\boldsymbol{u},\boldsymbol{v}) \tag{A1}$$

equal $-\infty$.

Proof. Without driving, the (ordinary) Lyapunov exponents are given as

$$\lambda_i=\lim_{n\to\infty}\frac{1}{nT}\ln(R^n_{ii}),$$

where R^n_{ii} $(i=1,\ldots,N)$ are the diagonal elements of the upper triangular matrix $\boldsymbol{R}^n$ that is obtained from a $\boldsymbol{QR}$ decomposition of the linearized flow

$$\boldsymbol{D}\phi^{nT}(\boldsymbol{u}_0,\boldsymbol{v}_0)=\boldsymbol{Q}^n\cdot\boldsymbol{R}^n. \tag{A2}$$

Here $\boldsymbol{Q}^n$ is an orthogonal matrix and T is some period of time. [Numerically the $\boldsymbol{QR}$ decomposition (A2) is computed iteratively using some suitable time step T.]

In the case of sporadic driving by means of a sequence $\boldsymbol{s}_T$ the flow $\phi^T=(\phi^T_{\boldsymbol{u}},\phi^T_{\boldsymbol{v}})$ has to be replaced by a map $\boldsymbol{G}$

$$(\boldsymbol{u}^{n+1},\boldsymbol{v}^{n+1})=\boldsymbol{G}^n(\boldsymbol{u}^n,\boldsymbol{v}^n,\boldsymbol{s}^{n+1})=(\boldsymbol{s}^{n+1},\phi^T_{\boldsymbol{v}}(\boldsymbol{u}^n,\boldsymbol{v}^n)),$$

with $\boldsymbol{s}^n=\boldsymbol{s}(nT)$, $\boldsymbol{u}^n=\boldsymbol{u}(nT)$ and $\boldsymbol{v}^n=\boldsymbol{v}(nT)$. The first k rows of the Jacobian matrix $\boldsymbol{DG}(\boldsymbol{u}^n,\boldsymbol{v}^n)$ equal zero. Therefore, also the first k rows of the Jacobian matrix of the n-fold iterated map $\boldsymbol{DG}^n(\boldsymbol{u}_0,\boldsymbol{v}_0)$ equal zero. Its $\boldsymbol{QR}$ decomposition $\boldsymbol{DG}^n(\boldsymbol{u}_0,\boldsymbol{v}_0)=\boldsymbol{Q}^n\cdot\boldsymbol{R}^n$ yields an upper triangular matrix $\boldsymbol{R}^n$ where again the first k rows vanish and thus $R^n_{ii}=0\Rightarrow\lambda_i=-\infty$ for $i=1,\ldots,k$.

[1] L.M. Pecora and T.L. Carroll, Phys. Rev. Lett. **64**, 821 (1990).
[2] R. He and P.G. Vaidya, Phys. Rev. A **46**, 7387 (1992).
[3] L. Kocarev and U. Parlitz, Phys. Rev. Lett. **74**, 5028 (1995).
[4] J.H. Peng, E.J. Ding, M. Ding, and W. Yang, Phys. Rev. Lett. **76**, 904 (1996).
[5] U. Parlitz, L. Kocarev, T. Stojanovski, and H. Preckel, Phys. Rev. E **53**, 4351 (1996).
[6] L. Kocarev, U. Parlitz, and T. Stojanovski, Phys. Lett. A **217**, 280 (1996).
[7] K. Cuomo and A.V. Oppenheim, Phys. Rev. Lett. **71**, 65 (1993).
[8] M.J. Ogorzalek, IEEE Trans. Circ. Syst. Part I **40**, 693 (1993).
[9] U. Parlitz and L. Kocarev, Int. J. Bifurcation Chaos **6**, 581 (1996).
[10] V.S. Afraimovich, N.N. Verichev, and M.I. Rabinovich, Radiophys. Quantum Electron. **29**, 795 (1986).
[11] N.F. Rulkov, M.M. Sushchik, L.S. Tsimring, and H.D.I. Abarbanel, Phys. Rev. E **51**, 980 (1995).
[12] L. Kocarev and U. Parlitz, Phys. Rev. Lett. **76**, 1816 (1996).
[13] S. Fahy and D.R. Hamann, Phys. Rev. Lett. **69**, 761 (1992).
[14] R.E. Amritkar and N. Gupte, Phys. Rev. E **47**, 3889 (1993).
[15] T. Stojanovski, L. Kocarev, and U. Parlitz, Phys. Rev. E **54**, 2128 (1996).
[16] P. Colet and R. Roy, Opt. Lett. **19**, 20 (1994).
[17] D.E. Sigeti, Physica D **82**, 136 (1995).
[18] J.G. Proakis, *Digital Communications* (Mc-Graw-Hill, New York, 1989).
[19] A. De Angeli, R. Genesio, and A. Tesi, IEEE Trans. Circ. Syst. Part I **42**, 54 (1995).
[20] H. Fujisaka and T. Yamada, Prog. Theor. Phys. **69**, 32 (1983).
[21] E. Ott and J.C. Sommerer, Phys. Lett. A **188**, 39 (1994).
[22] J.F. Heagy, T.L. Carroll, and L.M. Pecora, Phys. Rev. E **52**, R1253 (1995).
[23] D.J. Gauthier and J.C. Bienfang, Phys. Rev. Lett. **77**, 1751 (1996).
[24] B.R. Hunt and E. Ott, Phys. Rev. Lett. **76**, 2254 (1996).
[25] H.G. Schuster, S. Martin, and W. Martienesen, Phys. Rev. A **33**, 3547 (1986).
[26] J.F. Heagy, T.L. Carroll, and L.M. Pecora, Phys. Rev. Lett. **73**, 3528 (1994).
[27] J.C. Alexander, I. Kan, J.A. Yorke, and Z. You, Int. J. Bifurcation Chaos **2**, 795 (1992); J.C. Sommerer and E. Ott, Nature **365**, 138 (1993); E. Ott, J.C. Sommerer, J.C. Alexander, I. Kan, and J.A. Yorke, Phys. Rev. Lett. **71**, 4134 (1993); E. Ott, J.C. Alexander, I. Kan, J.C. Sommerer, and J.A. Yorke, Physica D **76**, 384 (1994).
[28] For a modification to definition 2 of asymptotic stability that ensompasses riddled basins, see J. Milnor, Commun. Math. Phys. **99**, 177 (1985).
[29] R. Brown, N.F. Rulkov, and E.R. Tracy, Phys. Lett. A **194**, 71 (1994).